Contract No:

This document was prepared in conjunction with work accomplished under Contract No. DE-AC09-08SR22470 with the U.S. Department of Energy.

Disclaimer:

Proceedings of the 12th International Conference on Environmental Remediation and Radioactive Waste Management
ICEM
October 11-15, 2009, Liverpool, UK

ICEM2009-16282

THE RESULTS OF TESTING TO EVALUATE CRYSTAL FORMATION AND SETTLING IN THE COLD CRUCIBLE INDUCTION MELTER

James Marra
Savannah River National Laboratory
Aiken, SC, USA

Sergey Stefanovsky
SIA Radon
Moscow, Russia

Dmitriy Suntsov
SIA Radon
Moscow, Russia

ABSTRACT

The Cold Crucible Induction Melter (CCIM) technology offers the potential to increase waste loading for High Level Waste (HLW) glasses leading to significant improvements in waste throughput rates compared to the reference Joule Heated Melter (JHM). Prior to implementation of a CCIM in a production facility it is necessary to better understand processing constraints associated with the CCIM. The glass liquidus temperature requirement for processing in the CCIM is an open issue. Testing was conducted to evaluate crystal formation and crystal settling during processing in the CCIM to gain insight into the effects on processing. A high aluminum/high iron content glass composition with known crystal formation tendencies was selected for testing. A continuous melter test was conducted for approximately 51 hours. To evaluate crystal formation, glass samples were obtained from pours and from glass receipt canisters where the glass melt had varying residence time in the melter. Additionally, upon conclusion of the testing, glass samples from the bottom of the melter were obtained to assess the degree of crystal settling. Glass samples were characterized in an attempt to determine quantitative fractions of crystals in the glass matrix. Crystal identity and relative composition were determined using a combination of x-ray diffraction (XRD) and scanning electron microscopy coupled with energy dispersive spectroscopy (SEM/EDS). Select samples were also analyzed by digesting the glass and determining the composition using inductively coupled atomic emission spectroscopy (ICP-AES). There was evidence of crystal formation (primarily spinels) in the melt and during cooling of the collected glass. There was evidence of crystal settling in the melt over the duration of the melter campaign.

INTRODUCTION

The CCIM offers the potential to increase waste loading for High Level Waste (HLW) glasses leading to significant improvements in waste throughput rates compared to the reference Joule Heated Melter (JHM). At the Savannah River Site (SRS) this could allow the Defense Waste Processing Facility (DWPF) to complete its mission earlier and enable faster closure of the SRS waste tanks.

An open issue remains regarding glass liquidus temperature (T_L) requirements for processing in the CCIM. The current specification for waste glass processing in the DWPF Joule Heated Melter (JHM) is the $T_{melt\ temp.} - T_L \geq 100°$ C. There appears to be no specific liquidus temperature criterion for CCIM processing and, in fact, previous tests were likely performed with the liquidus temperature of the glass *greater* than the melting temperature (suggesting that some volume percentage of crystals was processed through the melter during the demonstration) (1). In short-term testing this did not appear to be a problem. In longer-term operation, the potential for crystal settling and/or build-up in the melter must be considered as well as the potential for adverse effects on melter processing or operations (e.g. pouring). Therefore, a specific criterion for liquidus temperature needs to be established. Furthermore, an understanding of crystal formation and crystal settling for CCIM operations is needed.

EXPERIMENTAL

Glass Selection

Previously CCIM testing was conducted with the DWPF sludge batch 4 composition using Frit 503-R4 (Li_2O – 8 wt %, B_2O_3 – 16 wt %, SiO_2 – 76 wt %) at 50% waste loading on a calcined oxides basis. The SB4 composition is given in Table I. Isothermal liquidus temperature measurements (24 hours treatment at temperature) on this composition showed that a magnetite spinel phase was likely present at this temperature, however, the concentration was expected to be relatively low (Figure 1a). Liquidus temperature testing conducted on a glass at a waste loading of 55% indicated that the magnetite spinel was also present but at a higher concentration as evidenced by the relative intensity of the reflections in the x-ray diffraction (XRD) pattern (Figure 1b). Therefore, it was concluded that the testing to evaluate crystallization behavior in the CCIM should be conducted with the SB4 – Frit 503-R4 composition at a waste loading of 55 %.

Table I. Sludge Batch 4 Composition (calcined oxides basis)

Component	Calcined SB4 Waste
Al_2O_3	27.56
BaO	0.08
CaO	3.00
Cr_2O_3	0.22
CuO	0.05
Fe_2O_3	31.34
K_2O	0.08
MgO	3.00
MnO	6.25
Na_2O	20.22
NiO	1.80
PbO	0.41
SiO_2	2.93
ZnO	0.05
ZrO_2	0.10
F	0.02
Cl	1.59
I	0.04
P_2O_5	0.32
SO_3	0.94
Total	100.00

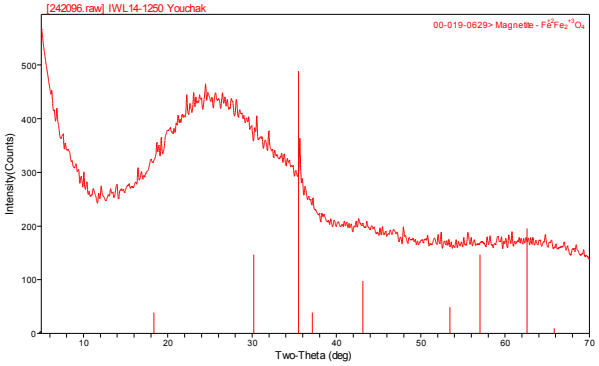

(a)

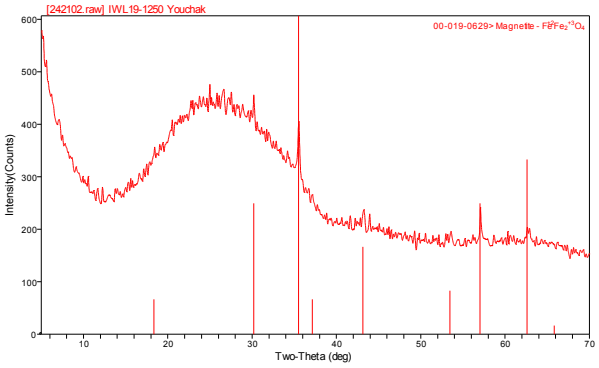

(b)

Figure 1. X-ray diffraction patterns for SB4-503-R4 glasses at (a) 50% waste loading and (b) 55% waste loading showing the presence of magnetite in these glasses after 24 hour isothermal treatment at 1250º C.

CCIM Testing

The CCIM tests were performed using the SIA Radon bench-scale facility (Figure 1) equipped with a 216 mm inside diameter cold crucible melter energized by a 60 kW power high frequency generator operated at frequency of 1.76 MHz supplied by a capacitor battery and a 295 mm copper inductor. The cold crucible (Figure 2) is a vessel of cylindrical shape with water-cooled walls and bottom. It is manufactured from stainless steel (Russian brand 12X18H10T) pipes. Sidewalls are fabricated from pipes 12 mm in diameter and 2 mm in thickness. Total crucible height is 521 mm, including the crucible itself – 500 mm, bottom – 16 mm, cover – 5 mm. The inner diameter is 216 mm which results in a melt surface area of 36,643 mm^2. The outside of the crucible walls is coated with protective zirconia-based putty. The cold crucible is equipped

with a pouring unit consisting of a water-cooled tube-in-tube cylinder with a blocking rod (gate) to stop glass pouring.

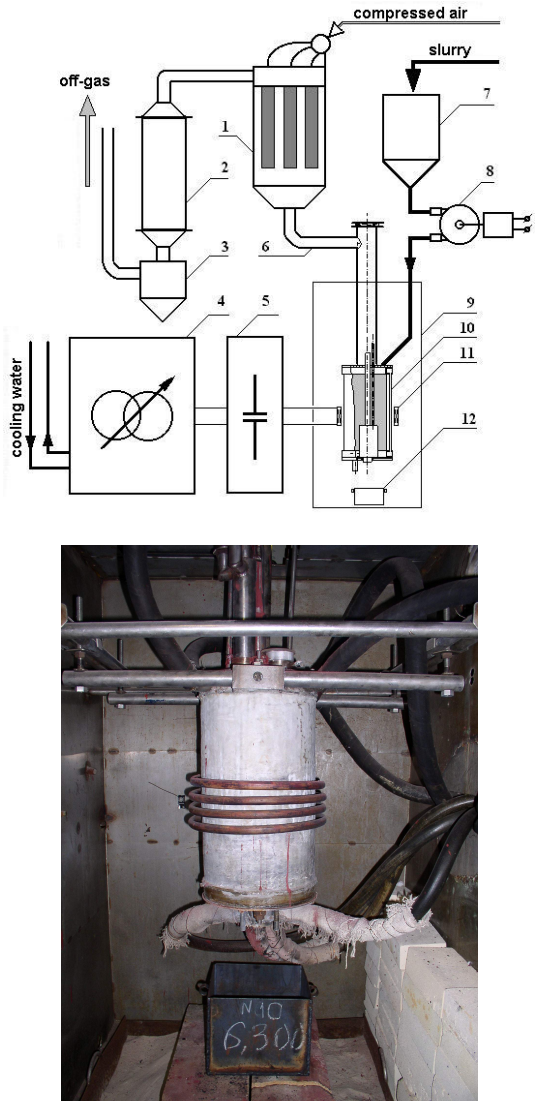

Figure 2. Schematic of the CCIM pilot-scale system (top) and installation of the cold crucible in the process box. 1- Filter, 2- Heat-exchanger, 3- Condensate collector, 4- High-frequency energizer, 5- Battery of capacitors, 6- Off-gas pipe, 7- Batch mixer, 8- Peristaltic pump, 9- Process box, 10- Cold crucible, 11- Inductor, 12- Container for glass.

The SB4 sludge surrogate (Table I) was prepared by adding appropriate concentrations of salts, hydroxides and oxides to produce a simulant that best mimics the actual waste. The surrogate was intermixed with Frit 503-R4 to result in a glass with a calcined oxides waste loading of 55% in a slurry with a water content of ~50 wt %.

The melter campaign was conducted in the following stages:

1 – Start-up of melter

2 – achieving steady state conditions with SB4 – 503-R4 composition

3 – tests to evaluate crystal formation/settling

4 – melter shutdown

During stage 3, feed was added to the melter and after feeding was stopped, the hold time in the melter was varied. The holding times were 30 minutes, 40 minutes, 64 minutes and 92 minutes. During each pour a sample was obtained from the melt stream and the bulk of the glass was captured in 10 L canisters. Each canister was sectioned both in the center and at the wall to obtain samples for analyses (Figure 3). The block samples were obtained in an attempt to assess heterogeneities within the glass melt since the varying locations in the canister represent different areas of the melter as the melter was drained. Comparison of samples in the center vs. the edge would provide as assessment of crystal formation as a function of cooling conditions since glass at the edge of the canister would cool significantly faster than glass in the center. Sampling of the dead volume and comparing to pour samples would provide a good indication in any crystal settling occurred over the duration of the campaign.

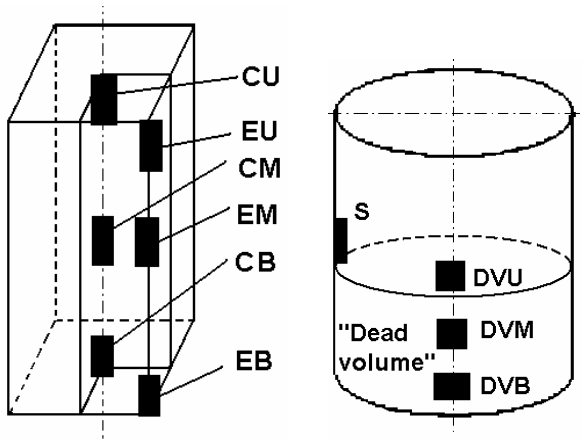

Figure 3. Schematic view of a section cut from the slowly glass block (left) and "dead" volume and skull layer in the cold crucible (right) and Sampling Areas. C – core, E – edge, U – upper part, M – middle part, B – bottom part, S – "skull", DV – "dead volume".

Sample Analyses

The glass samples that were obtained were analyzed by the following methods. X-ray diffraction was used for crystalline phase identification. Scanning electron microscopy coupled with energy dispersive spectroscopy (SEM/EDS) was used to examine the microstructure of the glasses and obtain chemical composition data. Metals, oxides and fluorides were used as

standards in the EDS analyses to facilitate quantitative chemical composition determination. Infrared spectroscopy (IR) was also performed on select glass samples to evaluate the glass structure. The relative crystal fraction in the samples was determined using image analysis software. Glass samples from the bulk of each canister and from the dead volume were also dissolved (sodium peroxide fusion and lithium-metaborate dissolution) and the dissolutions were analyzed using inductively coupled plasma atomic emission spectroscopy (ICP-AES).

RESULTS AND DISCUSSION

Melt stream samples were taken during each pour. Steel molds were used to obtain the samples. Due to the size of the molds (60 mm diameter x 40 mm depth), the glass cooled relatively quickly after sampling. There was clear evidence of crystal formation on the surface of the glass when examined visually (Figure 4). This is very typical of waste glasses at high waste loadings, due to the REDOX state of the glass at the air/glass interface after pouring. It should be noted that in many cases, this surface crystallization is not indicative of the bulk glass and in these cases the bulk glass is amorphous when examined using XRD. In this testing, XRD scans of the bulk glass from the pour samples (Figure 5) clearly indicated the presence of spinel (indexed to trevorite) and the objective of testing a glass that contained crystals within the melt appeared to be achieved. Furthermore, the XRD patterns for each of the samples were virtually identical indicating that crystallization within the glass was very similar irrespective of melt residence time.

Figure 4. Pour sample #1 obtained from the CCIM melt stream.

Infrared spectra of the glassy materials sampled from molds are shown in Figure 6. Within the high wavenumber range several bands due to stretching (valence: 3200-3600 cm^{-1}) and straining (deformation) O—H vibrations (1550-1750 cm^{-1}) in molecules of absorbed and structurally-bound water were present. The weak bands at 2750-2900 cm^{-1} were due to vibration of hydrogen bonds. Vibration of the bonds in the anionic motif of the glass network were responsible for the bands positioned lower than 1600 cm^{-1}. The strongest band at 1200-800 cm^{-1} was due to superposition of the bands due to O—Si—O vibrations in the SiO_4 units with various numbers of bridging oxygen ions connecting SiO_4 tetrahedra in the network: four (Q^4) – at ~1100-1150 cm^{-1}, three (Q^3) – at ~1050-1100 cm^{-1}, two (Q^2) – at ~1000-1050 cm^{-1}, one (Q^1) – at ~950-1000 cm^{-1}, and zero (Q^0) – at ~900-950 cm^{-1} (2-4). The bands with maxima at 1395–1410 cm^{-1} and ~1270 cm^{-1} were components of doubly degenerate asymmetric stretching, ν_3 O–B–O vibration in triangular BO_3 units. The bands at ~720 cm^{-1} and ~655 cm^{-1} were components of doubly degenerate asymmetric bending, δ_4, O–B–O vibrations (5). However taking into account the low boron content in the glassy material it should be suggested that major contribution to the band with a maximum at ~700 cm^{-1} was made by Al—O and ν_s O—Si—O vibrations. The latter are active in IR spectra if the symmetry of the SiO_4 units is lower than T_d (i.e. these units have one, two or three non-bridging oxygen ions). The shoulder at ~550 cm^{-1} was mainly due to Fe^{III}—O vibrations in both vitreous and spinel phases. The wavenumber range of 400-550 cm^{-1} corresponded to deformation vibrations in the SiO_4 units (2-4).

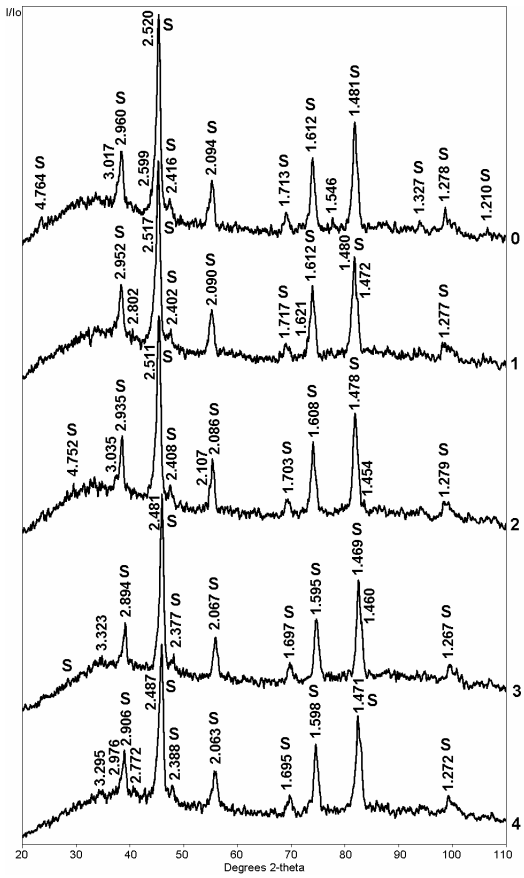

Figure 5. XRD spectra for samples poured in molds during each glass pour. Note: sample 0 was start-up glass. S=spinel.

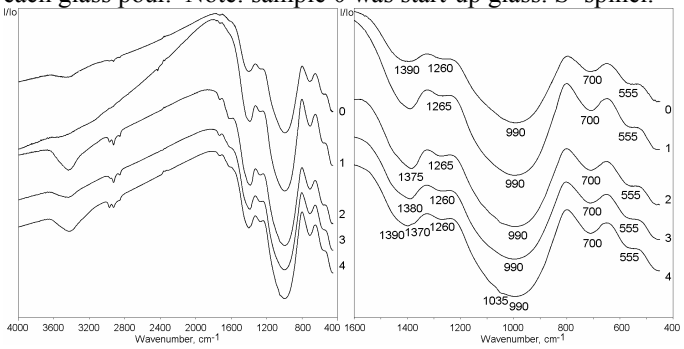

Figure 6. IR Spectra (left) and excerpt within the Range of 1600-400 cm^{-1} of the glass sampled from the molds.

The IR spectra of all the glasses were similar with only a few minor differences. In the spectra of the materials sampled from molds #2 and #4 the bands due to O—H and O—H··· vibrations had higher intensity than those in the spectra of other materials. The band with maximum ~1370-1390 cm^{-1} grew in intensity with regard to the band ~1260-1265 cm^{-1} pointing to contribution of different constituent to the first band, probably due to CO_3^{2-} ions. It appeared that at longer residence time in the cold crucible melter, a chemical differentiation in the melt appeared in the splitting of the broad band at 1200-800 cm^{-1} with formation of a higher wavenumber component (~1035 cm^{-1}) due to vibrations in the SiO_4 units with higher degree of connectedness probably forming metasilicate chains. The bands with maxima at ~700 and 555 cm^{-1} did not change their position and intensity confirming their attribution to vibrations of Al—O and Fe—O bonds because Al_2O_3 and Fe_2O_3 contents in the glassy materials remained the same.

The chemical analysis results for samples obtained from the canister bulk and from the dead volume of the melter indicated that settling of spinel crystals in the melter did occur over the duration of the run. Comparison of the analytical results for spinel forming species (Fe, Ni, Cr and Mn) in samples from the melter pours vs. glass obtained from the "dead volume" of the melter showed that the "dead volume" was enriched in spinel formers (Table II). The chemical analysis results indicated that there was little difference in the concentration of spinel formers (and other species) in the pour samples obtained for the varying melter soak times.

The interpretation of the results from the canister section samples was not straightforward. It was evident that the slow cooling resulted in an increase in the concentration of spinel phases in the glass. Also, the morphology of the spinel crystals varied from skelelton-type to more regular cubic shaped crystals. The cubic crystals were more often observed in samples from the centerline of the canister (Figure 7) coexisting with skeleton-type crystals while samples from the edge of the canister contained almost exclusively skeleton-type crystals (Figure 8). The glass in the center of the canister experienced slower cooling conditions likely leading to the formation of the more regular cubic shaped crystals.

Table II. Spinel Former Concentrations Determined by ICP-AES for Samples from Glass Pours and Melter

	Oxide Concentration (wt %)			
Sample ID	Fe_2O_3	NiO	Cr_2O_3	MnO
30 min	16.8	0.732	0.106	4.16
40 min	14.7	0.654	0.092	3.54
64 min	16.6	0.702	0.093	3.82
92 min	16.2	0.706	0.096	3.78
Dead Volume	26.3	2.42	0.492	4.87

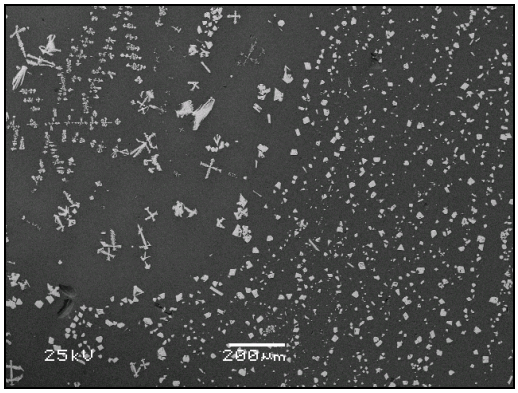

Figure 7. SEM image of glass from center-bottom of canister #5 (30 minute hold time) showing skeleton-type and cubic spinel crystals.

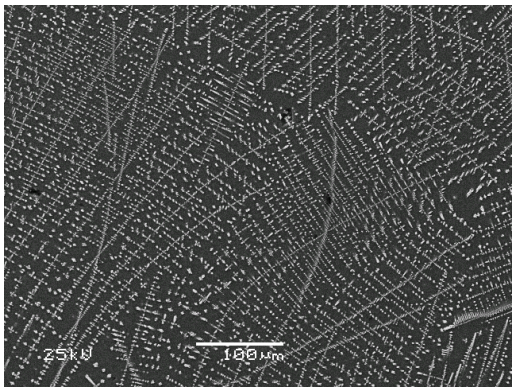

Figure 8. SEM image of glass from center-edge of canister #6 (40 minute hold time) showing skeleton-type crystals.

The morphology of the skeleton-type crystals and the amount of crystallization in the glass precluded the accurate

quantification of the crystalline fraction in the samples. Attempts to perform image analysis resulted in a high bias in areas where the skeleton-type crystals were present because the software could not readily discern the edges of the crystals.

Chemical analysis of the crystals using EDS indicated that the crystals were comprised of 4 oxygen ions with the sum of the cations very close to 3 indicative of the spinel AB_2O_4 structure. Table III provides the calculate formulae for several of the spinel crystals analyzed. These results were considered semi-quantitative due to the fact that the size of the electron beam diameter and the grain size were on the same order. However, it was apparent that the chemical formulae of the crystals were generally consistent and indicated that the crystals were a magnetite/trevorite solid solution.

EDS scans on areas of the samples were made in an attempt to discern chemical differences (i.e. relative enrichment or depletion of cations in the region) between samples from different areas of the canisters and between different holding time conditions. There was some indication that in some canisters, the bottom of the canisters were enriched in spinel formers (e.g. Fe). However, due to the analytical error associated with the EDS measurements this observation can not be considered conclusive. More quantitative analyses using wet chemistry methods may be useful in validating this tentative observation. Testing at longer residence times may also be useful in assessing the crystal settling behavior. However, long dwell times in the melter may result in volatility from the melt and change in the relative glass composition.

Table III. Chemical Formulae of Spinel Crystals in Select Samples

Hold Time (min)	Sample	Formulae
40	CB	$(Mg_{0.13}Mn_{0.20}Fe_{0.34}Ni_{0.33})^{2+}$ $(Cr_{0.03}Fe_{1.75}Al_{0.16})^{3+}O_4$
40	EU	$(Mg_{0.15}Mn_{0.25}Fe_{0.48}Ni_{0.12})^{2+}$ $(Cr_{0.03}Fe_{1.78}Al_{0.12})^{3+}O_4$
64	CM	$(Mg_{0.13}Mn_{0.19}Fe_{0.32}Ni_{0.36})^{2+}$ $(Cr_{0.04}Fe_{1.66}Al_{0.21})^{3+}O_4$
64	CB	$(Mg_{0.13}Mn_{0.18}Fe_{0.30}Ni_{0.39})^{2+}$ $(Cr_{0.05}Fe_{1.69}Al_{0.16})^{3+}O_4$
64	EU	$(Mg_{0.11}Mn_{0.18}Fe_{0.31}Ni_{0.40})^{2+}$ $(Cr_{0.11}Fe_{1.55}Al_{0.24})^{3+}O_4$
64	EU	$(Mg_{0.13}Mn_{0.22}Fe_{0.48}Ni_{0.17})^{2+}$ $(Cr_{0.02}Fe_{1.69}Al_{0.13})^{3+}O_4$
64	EB	$(Mg_{0.15}Mn_{0.18}Fe_{0.27}Ni_{0.40})^{2+}$ $(Cr_{0.08}Fe_{1.65}Al_{0.18})^{3+}O_4$
92	CU	$(Mg_{0.11}Mn_{0.18}Fe_{0.33}Ni_{0.38})^{2+}$ $(Cr_{0.06}Fe_{1.62}Al_{0.21})^{3+}O_4$
92	CM	$(Mg_{0.15}Mn_{0.25}Fe_{0.43}Ni_{0.17})^{2+}$ $(Cr_{0.01}Fe_{1.70}Al_{0.14})^{3+}O_4$
92	CB	$(Mg_{0.11}Mn_{0.21}Fe_{0.42}Ni_{0.26})^{2+}$ $(Cr_{0.02}Fe_{1.69}Al_{0.14})^{3+}O_4$
92	EB	$(Mg_{0.12}Mn_{0.19}Fe_{0.31}Ni_{0.37}Zn_{0.01})^{2+}$ $(Cr_{0.05}Fe_{1.61}Al_{0.25})^{3+}O_4$

CONCLUSIONS

The testing to evaluate crystallization behavior in the CCIM resulted in the following conclusions:

- The selected composition resulted in crystallization in the melter as evidenced by spinel crystals in samples obtained from the melt pour stream.
- Crystallization in the glass was accentuated by the slow cooling conditions experienced in the glass receipt canisters.
- The morphology of the crystals in the slowly cooled glass was influenced by the degree of slow cooling.
- Chemical analyses on digested glass samples clearly showed that spinel crystals settled in the melter over the course of the melter campaign.
- The chemistry and quantity of crystals were generally independent of soak time in the melter. The crystals were identified as a magnetite/trevorite solid solution.

ACKNOWLEDGMENTS

The work was performed under financial support from U.S. Department of Energy - Office of Environmental Management. Authors are grateful to Mr. Kurt Gerdes for his support of this project.

REFERENCES

1. A.P. Kobelev, S.V. Stefanovsky, V.V. Lebedev, M.A. Polkanov, V.V. Gorbunov, A.G. Ptashkin, O.A. Knyazev and J. C. Marra, "Full-scale Cold Crucible Test on Vitrification of Savannah River Site SB4 HLW Surrogate," **Ceramic Transactions**, American Ceramic Society, Westerville, OH, in press.
2. K. Nakamoto, **Infrared Spectra of Inorganic and Coordination Compounds**, John Wiley & Sons, New York, London (1962).
3. I.I. Plusnina, **Infrared Spectra of Minerals**, MGU, Moscow (1977).
4. V.N. Anfilogov, V.N. Bykov, A.A. **Osipov, Silicate Melts**, (Russ.), Nauka, Moscow (2005).
5. V.A. Kolesova, "Vibrational Spectra and the Structure of Alkali Borate Glasses," **Glass Physics and Chemistry** (Russ.) **12** [1] (1986) 4-13.